Sedimentology (2001) **48,** 57–78

Long-distance correlation between tectonic-controlled, isolated carbonate platforms by cyclostratigraphy and sequence stratigraphy in the Devonian of South China

DAIZHAO CHEN*†, MAURICE E. TUCKER†, MAOSHENG JIANG* and JINGQUAN ZHU*
**Institute of Geology and Geophysics, Chinese Academy of Sciences, PO Box 9825, Beijing 100029, P.R. China (E-mail: dzh.chen@mail.igcas.ac.cn)*
†Department of Geological Sciences, University of Durham, Durham DH1 3LE, UK (E-mail: m.e.tucker@durham.ac.uk)

ABSTRACT

During the early Middle Devonian in South China, an extensive carbonate platform was broken up through extension to create a complex pattern of platforms, and interplatform basins. In Givetian and Frasnian carbonate successions, five depositional facies, including peritidal, restricted shallow subtidal, semi-restricted subtidal, intermediate subtidal and deep subtidal facies, and 18 lithofacies units are recognized from measured sections on three isolated platforms. These deposits are arranged into metre-scale, upward-shallowing peritidal and subtidal cycles. Nine third-order sequences are identified from changes in cycle stacking patterns, vertical facies changes and the stratigraphic distribution of subaerial exposure indicators. These sequences mostly consist of a lower transgressive part and an upper regressive part. Transgressive packages are dominated by thicker-than-average subtidal cycles, and regressive packages by thinner-than-average peritidal cycles. Sequence boundaries are transitional zones composed of stacked, high-frequency, thinner-than-average cycles with upward-increasing intensity of subaerial exposure, rather than individual, laterally traceable surfaces. These sequences can be further grouped into catch-up and keep-up sequence sets from the long-term (second-order) changes in accommodation and vertical facies changes. Catch-up sequences are characterized by relatively thick cycle packages with a high percentage of intermediate to shallow subtidal facies, and even deep subtidal facies locally within some individual sequences, recording long-term accommodation gain. Keep-up sequences are characterized by relatively thin cycle packages with a high percentage of peritidal facies within sequences, recording long-term accommodation loss. Correlation of long-term accommodation changes expressed by Fischer plots reveals that during the late Givetian to early Frasnian increased accommodation loss on platforms coincided with increased accommodation gain in interplatform basins. This suggests that movement on faults resulted in the relative uplift of platforms and subsidence of interplatform basins. In the early Frasnian, extensive siliceous deposits in most interplatform basins and megabreccias at basin margins correspond to exposure disconformities on platforms.

Keywords Cyclostratigraphy, Frasnian, Givetian, high-frequency cyclicity, isolated platforms, platform carbonate correlation, South China.

INTRODUCTION

Metre-scale, upward-shallowing cycles (or parasequences) are the basic building units of thick shallow-water carbonate successions throughout the Phanerozoic and are commonly organized into relatively large-scale depositional sequences. Thick shallow-water carbonate successions are characterized by a hierarchy of stratigraphic cyclicity (e.g. Goldhammer *et al.*, 1990, 1993; Elrick & Read, 1991; Osleger & Read, 1991; Montañez & Read, 1992; Montañez & Osleger, 1993; Elrick, 1995; Balog *et al.*, 1997; Strasser & Hillgärtner, 1998).

Many studies have documented Devonian platform carbonate cycles and sequences from around the world (e.g. Read, 1973; Wong & Oldershaw, 1980; Goodwin & Anderson, 1985; Dorobek, 1991; McLean & Mountjoy, 1994; Elrick, 1995, 1996; Yang *et al.*, 1995; Garland *et al.*, 1996; Lamaskin & Elrick, 1997). Sequence development and the history of relative sea-level change in the Devonian strata of South China have been documented (Chen & Chen, 1994a,b; 1995; Shen *et al.*, 1994; Du *et al.*, 1996; Gong *et al.*, 1997), but detailed studies of the high-frequency cyclicity of platform carbonates have not been carried out. There is still much difficulty in correlating the platform strata because of insufficient biostratigraphic control.

This paper aims to: (1) describe and interpret depositional environments of upper Middle and Upper Devonian carbonates across different platforms in Guangxi and Hunan provinces, South China; (2) demonstrate different cycle types and their possible links to eustatic sea-level changes; (3) illustrate the cycle stacking patterns of individual stratigraphic sections, and integrate these with sedimentological, stratigraphical and diagenetic features to identify and correlate depositional sequences across the study area; and (4) document the interaction between tectonics and eustasy, and determine their control on cycle and sequence development, and platform evolution.

PALAEOGEOGRAPHY AND STRATIGRAPHY

As a result of the 'Guangxi' (Caledonian) Orogeny at the end of the Silurian, marine waters receded from much of the Yangtze Plate. In South China, the sea only persisted from Silurian into Devonian times in southern Guangxi along a narrow belt named the Qinfang Trough (Wu *et al.*, 1987; Zhong *et al.*, 1992). The greatly enlarged landmasses formed by the orogeny created a complex topography, which exerted a fundamental influence on the subsequent Devonian depositional systems, in conjunction with the reactivation of basement fault zones.

From the beginning of the Devonian, marine waters gradually transgressed from the southwest to the northeast, reaching their farthest extent in the Frasnian. In the early Givetian, the carbonate depositional area expanded considerably, and clastics retrograded to a very narrow area close to the uplands. From late Givetian to early Frasnian times, the carbonate platforms underwent intense fragmentation, and two major sets of interplatform basin were formed, intersecting in central Guangxi (Fig. 1). The interplatform basins in western Guangxi were dominantly oriented NW–SE, and show a grid-like pattern (Chen & Zeng, 1990; Zhang & Zheng, 1990; Zeng *et al.*, 1992, 1995; Liu *et al.*, 1993; Liu, 1998). By contrast, those in eastern Guangxi and Hunan mainly striked in a NNE–SSW direction, and show some features of a strike-slip system (Shen *et al.*, 1987; Jiang, 1990; Zeng *et al.*, 1992; Liu *et al.*, 1993; Liu, 1998). The formation of this Devonian platform-basin system in South China was probably related to a transform fault extending into the continental margin during the opening of Palaeo-Tethys (Chen & Zeng, 1990; Zeng *et al.*, 1992, 1995; Liu *et al.*, 1993; Liu, 1998).

This study will focus on the platform carbonates of Givetian and Frasnian age; namely the Mintang and Rongxian (in part) formations in the Litang area of south-central Guangxi, the Tangjiawan (locally with Mintang), Guilin and Dongcun (in part) formations in the Guilin area, and the Qiziqiao Formation in central Hunan (Fig. 2). These formations are conformable on lower Middle Devonian carbonates in south-central Guangxi and terrigenous clastics in northern Guangxi and Hunan Provinces, and are overlain by Fammenian carbonates. On the basis of biostratigraphy, these formations approximately correspond to the Givetian and Frasnian (Tan *et al.*, 1987; Wu *et al.*, 1987; Zhong *et al.*, 1992; BGMR of Hunan, 1997); the correlation between the formations is given in Fig. 2.

DEPOSITIONAL FACIES

Five major outcrops were examined on three isolated platforms in Hunan and Guangxi Provinces: Ma'anshan (MA) and Xizhaikou (XZ) on

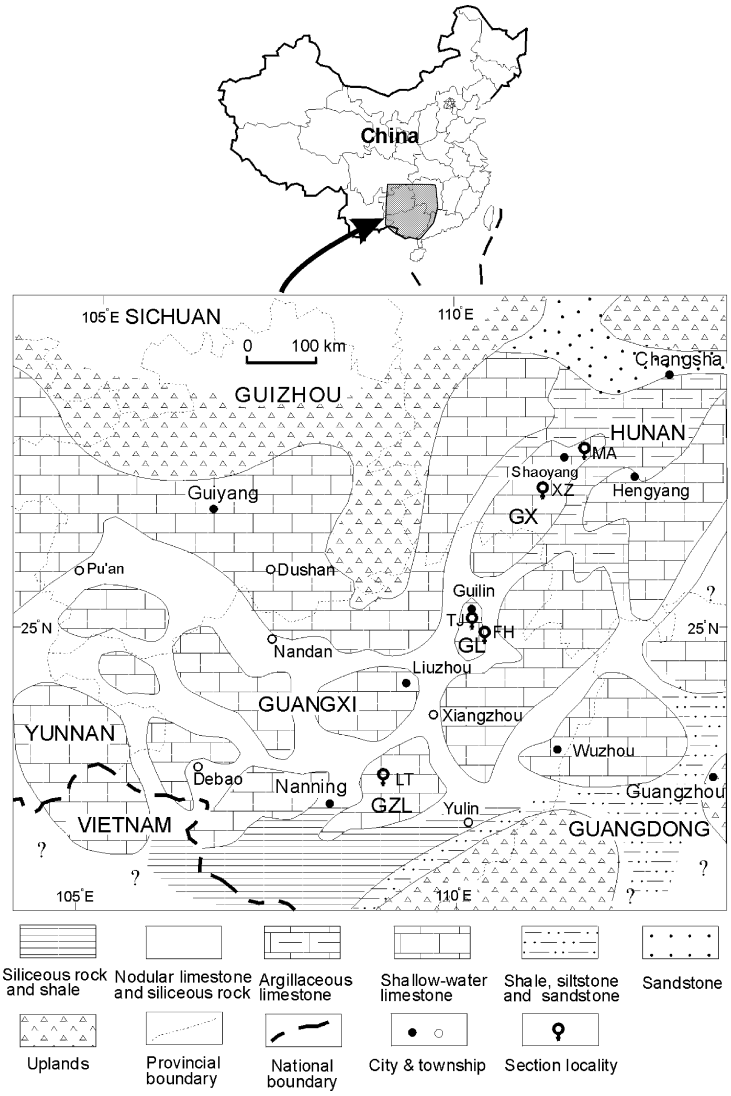

Fig. 1. Palaeogeographic setting of South China in the Frasnian. The area was characterized by a complex pattern of platforms and interplatform basins created by intense synsedimentary block-faulting in approximately NNE–SSW and NW–SE directions. Localities: MA, Ma'anshan; XZ, Xizhaikou; TJ, Tangjiawan; FH, Fuhe; LT, Litang. Platforms: GX, Guibei-Xiangzhong Platform; GL, Guilin Platform; GZL, Guizhong-Litang Platform.

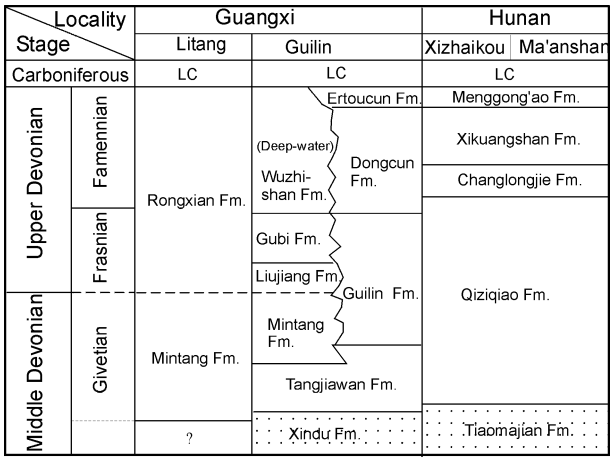

Fig. 2. Lithostratigraphic units of the Middle and Upper Devonian platform carbonate successions in Guangxi and Hunan Provinces. LC, Lower Carboniferous. Stipple indicates terrigenous clastic formations below the studied interval.

the Guibei-Xiangzhong (GX) platform; Tangjiawan (TJ) and Fuhe (FH) on the Guilin (GL) platform; Litang (LT) on the Guizhong-Litang (GZL) platform (see Fig. 1 for location). Continuous measured sections were obtained for each outcrop. Eighteen lithofacies types were identified in the Givetian and Frasnian, and these are arranged into five major depositional facies. In order of increasing relative water depth they are: peritidal, restricted-shallow subtidal, semi-restricted subtidal, intermediate subtidal, and deep subtidal/basinal facies (Table 1). In the platform carbonate successions, high-frequency metre-scale, upward-shallowing peritidal and subtidal cycles (fourth- to fifth-order parasequences) can be identified by the vertical facies arrangements. These small-scale cycles can be further arranged into larger-scale depositional sequences (tens to hundreds of metres thick).

Table 1. Summary of depositional facies of Givetian and Frasnian carbonate strata, South China.

Lithofacies unit + thickness	Lithology	Sedimentary structures/textures	Biota	Interpretation	Occurrence
Peritidal facies					
Planar laminite (0·05–0·4 m)	Alternating Ms/peloidal Ps (or Ws), or dolo-Ms/dolosiltite	Millimetre-scale planar or smooth (crinkly locally) laminae; flat intraclasts; desiccation cracks, dissolution cavities locally	Rare with calcispheres	Upper intertidal to supratidal	Lower part of Qiziqiao Fm, Rongxian Fm, rare in Guilin Fm
Wavy laminite (0·05–2·5 m)	Alternating peloidal Ps (or Ws)/(crypt-) microbialite; intergrown (crypt-) microbialite or cryptmicrobialite/ microbialite	Centimetre-scale undulatory laminae, domal laminae or LLH stromatolites intercalated locally; fenestrae locally; inhomogeneous dolomitiztion	*Amphipora,* ostracods, gastropods; *Epiphyton* or *Angulocellularia, Rothpletzella, Ursoscupulus,* calcispheres	Lamination most likely microbial origin with abundant cyano-bacteria; shallow subtidal to intertidal	Minor in Tangjiawan Fm and equivalents; abundant in other fms
Fenestral limestone (>0·1 m)	Fenestral peloidal Ms to Ps, rare Gs	Laminoid, irregular and tubular fenestrae common, spherical ones rare; geopetal fabrics common; weak lamination in laminoid fenestral zones	Ostracods, gastropods, calcispheres, *Amphi-pora* common; minor parathuramminid foraminifera	Shallow subtidal to intertidal	Dongcun Fm, Upper Mb of Guilin Fm, uppermost Qiziqiao Fm
Pedogenic/meteoric altered unit (0·02–0·4 m)	Originally subtidal through supratidal lithology; pedogenic claystone/siltstone	Rubble or cinder-like fabrics, fitted argillaceous seams; laminated crusts; reddening locally; fabrics related to dissolution (cavities/ pipes, neptunian dykes or cracks, microkarstic relief); rare alveolar septal textures; vadose cements	Barren; rare root moulds	Subaerially exposed tidal flat through shallow subtidal facies	Limited horizons in Upper Mb of Guilin Fm, Rongxian and Qiziqiao fms
Restricted shallow subtidal facies					
Stromatolite Bs (0·2–0·5 m)	Alternating peloidal Ps (or Ws)/cryptmicrobial micrites; intergrown (crypt-)microbialites; usually intercalated in wavy laminites	Lateral-linked hemispheric (LLH) laminae (10–35 cm wide, 5~10 cm tall) common, stacked hemispheric (SH) (or digitate, columnar) rare	Ostracods and gastropods, rare *Amphipora*	Restricted, shallow subtidal to lower intertidal	Rongxian Fm, Lower Mb of Guilin Fm

Peloidal Gs/Ps (0·2–1·5 m)	Peloidal Ws through Gs with minor bioclastics and sparse (lumpy) intraclasts	Fenestrae locally; rare weak lamination	Ostracods, foraminifera, calcispheres common, sparse *Amphipora* and brachiopods	Very shallow subtidal, intertidal shoals or tidal creeks	All fms except Tangjiawan Fm
Oolitic Gs (0·2–1·0 m)	Oolitic Gs/Ps with subordinate peloids and bioclasts	Rare graded grains; radial and superficial ooids dominant, relatively well-sorted; microfenestral fabrics	Sparse ostracods and calcispheres	Very shallow subtidal to intertidal creeks	Rare in Qiziqiao and Rongxian fms
Amphipora Fs/Ps (0·2–3·5 m)	*Amphipora* Fs (or Ws)/ Ps and Gs locally	Broken *Amphipora,* randomly aligned to parallel-preferred orientation; locally intercalated in microbial laminites	*Amphipora* dominant, sparse ostracods, gastropods, foraminifera and stromatoporoids; bioturbation	Restricted, shallow subtidal without strong current agitation	All fms except Rongxian Fm at Litang
Bioturbated Ms/Ws (0·2–1·5 m)	Bioturbated Ms/Ws with peloidal Ps/Gs lenses	Massive, mottled appearance, anastomosed burrow networks; selective dolomitization	Rare ostracods, gastropods and spheroidal foraminifera (i.e. umbellids)	Restricted to semi-restricted shallow subtidal	Absent in Tangjiawan Fm
Fossil-poor Ms (0·2–1·0 m)	Fossil-poor Ms, argillaceous seams	Thin-to medium bedded, nodular bedding locally	Rare thin-shelled ostracods, gastropods and umbellid foraminifera	Restricted, quiet shallow subtidal	Common in Qiziqiao and Guilin fms
Semi-restricted subtidal facies					
Ostracod Ps/Gs (0·2–0·5 m)	Ostracod Ps/Gs with minor gastropods, bivalve shells and peloids	Thin-to medium-bedded; intercalated in stromatoporoid Bs; disarticulated and abraded shells	Ostracods dominant, minor gastropods, bivalves	Semi-restricted, storm-reworked deposits or shoals behind biostromes	Tangjiawan Fm
Gastropod Ws/Ps (0·2–0·8 m)	Gastropod Ws/Ps, thin argillaceous seams intercalated	Thin-bedded; graded and locally preferred orientation; rare shelter fabrics	Abundant gastropods, minor ostracods and tubular foraminifera, rare tentaculitid shells	Storm-redeposited in semi-restricted deep lagoon or intraplatform basin	Lower part of Mintang Fm at Fuhe
''Tentaculitid'' Ws/Ps (0·2–4 m)	Tentaculitid-like Ws/Ps	Thin- to thick-bedded, weakly oriented tubiform shells	Tentaculitid-like fauna with thick walls dominant; minor ostracods, gastropods, foraminifera	Semi-restricted deep lagoon on platforms	Upper Mb of Guilin Fm

Table 1 (Continued).

Lithofacies unit + thickness	Lithology	Sedimentary structures/textures	Biota	Interpretation	Occurrence
Intermediate subtidal facies					
Stromatoporoid (dolo-) Bs (0·5–15 m)	Stromatoporoid Fs/Rs (minor Bi), tabular stromatoporoid Fs/Ba; skeletal Ws/Ps matrix; strongly dolomitized locally (especially in Tangjiawan Fm and equivalents)	Massive to thick-bedded; rare domal shape in relief; overturned stromatoporoids common, *in situ* growth position rare	Bulbous, hemispherical, platy/tabular, branching stromatoporoids; corals, brachiopods, gastropods, foraminifera, rare bryozoans and crinoids; bioturbation	Open-marine, moderately deep subtidal; platform interior biostromes (or bioherms); not strong wave resistant structures	In all strata, but quite abundant in Tangjiawan Fm and equivalents
Skeletal Ws/Ms (0·2–2·0 m)	Diversified skeletal Ws/Ms; sparse argillaceous seams intercalated	Thin- to medium-bedded	Brachiopods, corals, stromatoporoids, gastropods, crinoids, echinoids, bryozoans, rare tentaculitids	Open-marine, moderate to deep subtidal; near or below fair-weather wave base	Tangjiawan Fm, lower part of Qiziqiao Fm
Deep subtidal/basinal facies					
Nodular skeletal Ws/Ms (0·1–2·0 m)	Argillaceous skeletal Ws/Ms	Nodular-bedded; abraded skeletal grains	Diversified brachiopods, rugose corals, crinoids, gastropods, bryozoans; rare tentaculitids; *Thalassinoid*-type burrows	Open-marine, deep subtidal; below fair-weather wave base, episodic storm agitation	Tangjiawan Fm, lower part of Qiziqiao Fm
Tentaculitid Ms/Ws intercalated with argillites (0·2–4·0 m)	Tentaculitid Ms/Ws, intercalated with thin argillaceous beds or seams; high organic matter; cherty nodules or bands (Liujiang Fm only)	Thin-bedded; upward-thickening bedding patterns	Thin-shelled tentaculitids; minor brachiopods, calcisponges, gastropods, foraminifera	Very deep subtidal to interplatform basin	Mintang Fm, lower part of Liujiang Fm

Ms, mudstone; Ws, wackestone; Ps, packstone; Gs, grainstone; Bs, boundstone; Bi, bindstone; Ba, bafflestone; Fs, floatstone; Rs, rudstone; Fm, Formation; Mb, Member.

These depositional sequences were recognized and correlated by cycle stacking patterns, and vertical facies trends combined with subaerial exposure features traceable across the different platforms.

Peritidal facies

Peritidal facies include planar laminite, wavy laminite, fenestral limestone and minor pedogenic and meteoric-altered units (Table 1). Planar laminites and wavy laminites (Fig. 3A) form caps to peritidal cycles and thin transgressive bases to some peritidal cycles. Within the fenestral limestones, four fenestral types occur: laminoid, irregular, tubular and spherical. Irregular (or tubular) fenestral limestones commonly grade into laminoid ones, constituting upward-shallowing cycles.

Pedogenic/meteoric-altered units form the caps of cycles with host substrates either of peritidal or shallow subtidal facies. Karstic processes appear to have dominated over pedogenic processes, and common features include *in situ* breccias (rubble) (Fig. 4A and B), dissolution cracks and fills, and terra-rossa-type soils (Fig. 4C and D), with rare laminated crusts.

In situ breccias can reach 40 cm in thickness and are light pink-grey to dark brown in colour; their transition to the substrate is gradual, similar to the regolith illustrated by Szuczewski *et al.* (1996; fig. 3C and D). The breccias consist of cm-sized clasts of host rock either of peritidal facies, such as laminite and lime mudstone (peritidal pond deposit), or shallow subtidal facies such as *Amphipora* floatstone/wackestone. Their matrix is a greenish to red dolomitic clay. Densely packed clasts are generally irregular to subrounded in shape, with fitted ferruginous rims in some cases (Fig. 4B). Vadose cements are common. The brecciation is probably related to periodic wetting and drying during subaerial exposure.

Dissolution depressions and pipes, anastomosing cracks and veins (Fig. 4C and D), and neptunian dykes are found at subaerial exposure horizons. Dissolution residues of siltstone occur within the dissolution depressions, and dissolution pipes below are filled with coarse blocky calcite. Anastomosing cracks in brecciation zones are filled with granular ferroan calcite or dolomite, with some geopetal texture. Alveolar septal texture is observed locally along the cracks and possibly related to microbial activity around root systems. Some cracks are downward tapering, and range in width up to tens of centimetres and in depth up to 1·5 m. They are filled with subtidal deposits of the overlying units, locally with brownish to purple terra-rossa claystone at the bottom.

Clayey palaeosols form the top section of subaerial exposure-affected horizons (Fig. 4D).

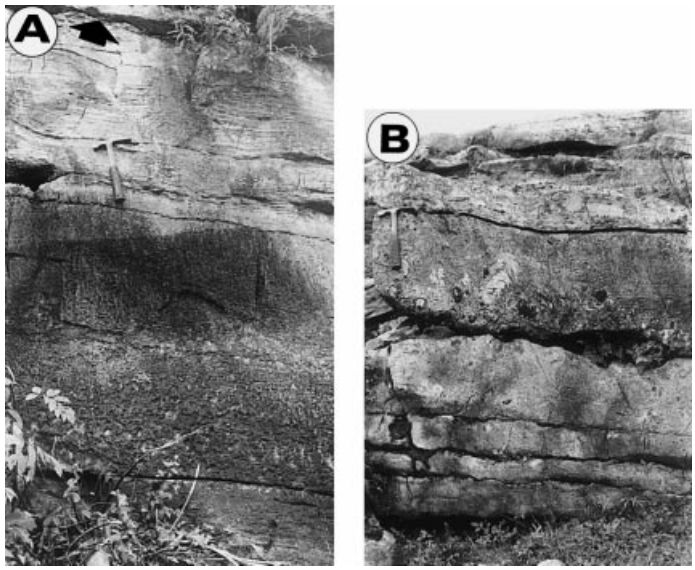

Fig. 3. Common facies and cycle types in the study area. (A) Peritidal cycle. Mottled, bioturbated mudstone/wackestone is covered by undulatory microbial laminite. See the network of irregular burrows in the lower part. The cycle boundary is indicated by an arrow. Hammer for scale (37 cm long). Guilin Formation, Tangjiawan, Guilin. (B) Subtidal cycle. Thin- to medium-bedded skeletal wackestone/mudstone at the base changes into stromatoporoid floatstone/wackestone upwards; bulbous and columnar stromatoporoids are in their growth position. The black line marks the cycle top. Hammer for scale (37 cm long). Qiziqiao Formation, Xizhaikou, Shaoyang County, Hunan.

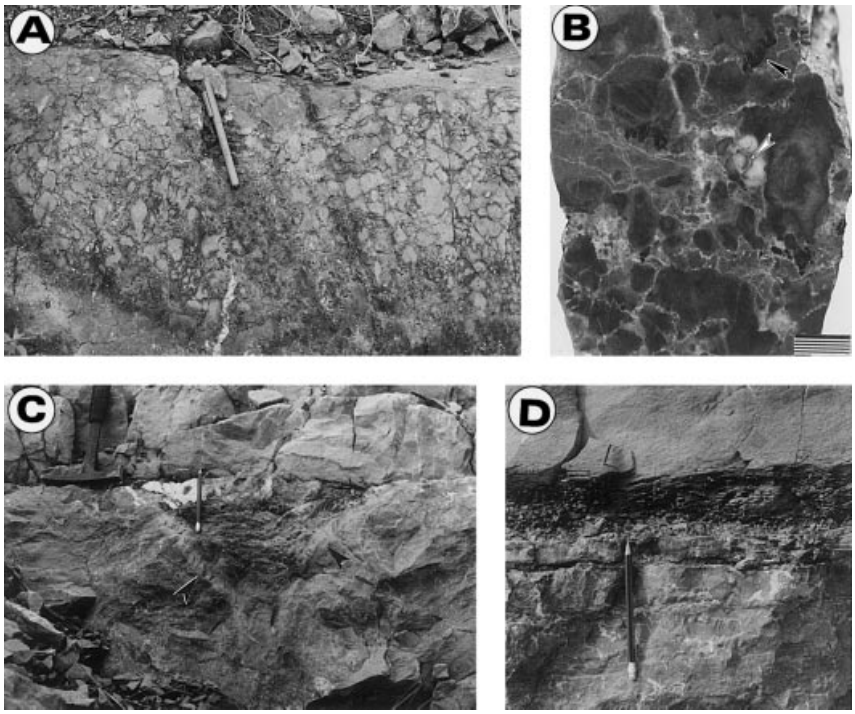

Fig. 4. (A) Brecciation during subaerial exposure. Note the cinder-like rubble coated with purple dolomitic argillaceous seams. The original rock is *Amphipora* wackestone/mudstone, which is also reddened. Pen is 14 cm long. Guilin Formation. Tangjiawan, Guilin. (B) Polished slab from (A). Subangular to subrounded, red to purplish, *in situ* clasts are coated with brownish, ferruginous crust. Black pebbles are also present (black arrow). Cavities are filled by blocky calcite with minor pendant calcite cements (white arrow). Matrix is dolomitic argillaceous mudstone. Scale bar is 1 cm long. (C) Funnel-shaped dissolution pit with insoluble residue (dolomitic siltstone). The light-coloured walls (arrowed) with numerous dissolution veins beneath, are the result of leaching during subaerial exposure. Pencil is 13·5 cm long. Rongxian Formation, Litang, Guangxi. (D) An exposure profile showing the transition from unaltered host rock to a brecciated zone with anastomosing veins and cavities, via an argillaceous brecciated zone, and finally to the dark greenish dolomitic siltstone/silty shale. The veins and cavities are filled with granular dolomite spar. The pencil is 14 cm long. Rongxian Formation, Litang, Guangxi.

They are generally 5–20 cm thick, grey to yellowish green in colour, and illite dominated. Rare root moulds have been observed. In some cases, calcareous nodules occur within the claystone. Such clay soils are documented in Cretaceous and Triassic peritidal cycles and reflect a relatively humid climate during emergence (Deconinck & Strasser, 1987; Strasser, 1988; Balog *et al.*, 1997).

Rare laminated pedogenic crusts form the caps to fenestral limestones. They are light grey to pink in colour and 2 cm to 10 cm in thickness, and consist of fine laminae composed of micrite with coated grains and peloids, along which greenish clayey bands are distributed.

Restricted shallow subtidal facies

Restricted shallow subtidal facies include: (1) stromatolite boundstone; (2) peloidal grainstone/packstone; (3) oolitic grainstone; (4) *Amphipora* floatstone/packstone; (5) bioturbated mudstone/wackestone; and (6) fossil-poor mudstone/wackestone (Table 1). Stromatolite boundstones are commonly present below, or intercalated with microbial laminites. They are commonly nucleated on scoured surfaces and intraclasts. Peloidal grainstones/packstones form the lower or middle parts of peritidal cycles, and commonly grade upwards into fenestral limestones or microbial laminites. The rare oolitic grainstones are located in the lower or middle part of peritidal cycles, and generally grade into fenestral limestones or microbial laminites. The common *Amphipora* floatstones/packstones form the lower or middle parts of peritidal cycles or the cap to subtidal cycles. They are characterized by mono-specific spaghetti-like *Amphipora* stromatoporoids. Bioturbated mudstones/wackestones (middle of Fig. 3A) form the lower or middle part of both peritidal cycles and subtidal cycles. Fossil-poor mudstones form the lower parts of peritidal

cycles or caps to subtidal cycles. Similar subtidal facies have been described by Dorobek (1991), Elrick (1995, 1996), Garland *et al.* (1996) and Lamaskin & Elrick (1997).

Semi-restricted subtidal facies

This less common facies association includes: ostracod packstone/grainstone, gastropod wackestone/packstone and 'tentaculitid' wackestone/packstone (Table 1). The 'tentaculitid' wackestones/packstones form the base of subtidal cycles (Fig. 5D), and are characterized by tentaculitid-like shells (25–50% of the bioclasts) with a relatively thick wall, suggesting a nekto-benthic lifestyle.

Intermediate subtidal facies

Intermediate subtidal facies include: stromatoporoid (dolo-) boundstone and skeletal wackestone/mudstone (Table 1). Stromatoporoid (dolo-) boundstones form the lower or middle parts of subtidal cycles and peritidal cycles. Two sublithofacies: stromatoporoid floatstone/rudstone and platy/tabular stromatoporoid floatstone/bafflestone can be recognized (Table 1), with the latter generally grading into the former. Skeletal

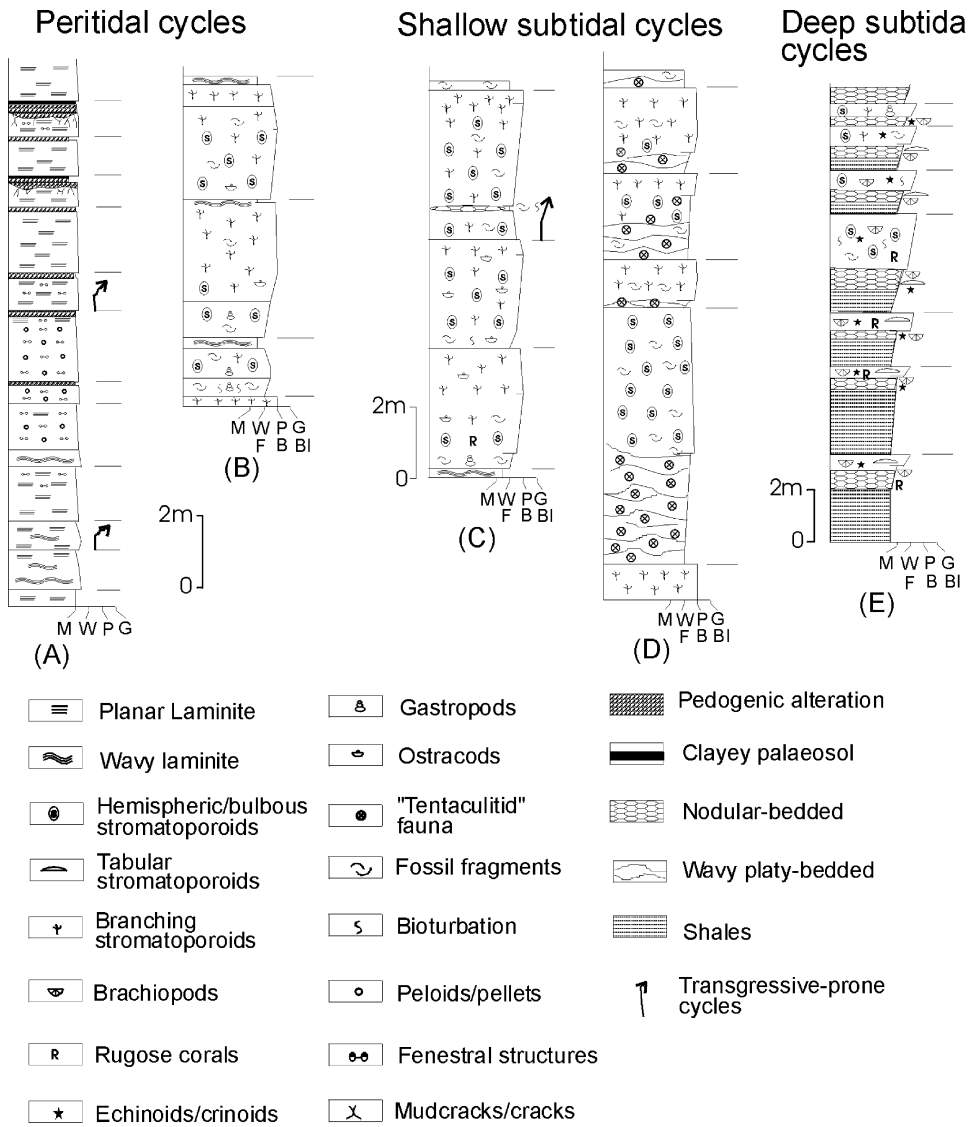

Fig. 5. Common cycle types in the study area. (A, B) Peritidal cycles; (C, D) shallow subtidal cycles; and (E) deep subtidal cycles. Bounding surfaces of cycles are marked by short lines on the right sides of logs. A, Litang; B–D, Tangjiawan; E, Ma'anshan. M, mudstone; W, wackestone; P, packstone; G, grainstone; F, floatstone; B, bafflestone; BI, bindstone.

wackestones/mudstones form the base or middle parts of some subtidal cycles.

Deep subtidal facies

Deep subtidal facies include nodular skeletal wackestone/packstone and tentaculitid mudstone/wackestone intercalated with argillite (Table 1). Nodular skeletal wackestones/mudstones are normally present at the base or in the lower part of subtidal cycles. Tentaculitid mudstones/wackestones intercalated with argillites form cycles several metres thick, displaying upward-increasing bed thickness.

CARBONATE PLATFORM DEPOSITIONAL MODEL

The Devonian platforms in South China are mostly isolated carbonate platforms, with rare clastic influxes trapped within interplatform basins (e.g. Shen *et al.*, 1987; Wu *et al.*, 1987; Zhong *et al.*, 1992). The topography of the isolated platforms was variable, but generally with a sharp transition from platform to basin, particularly those in western Guangxi. Platforms like GX, GL and GZL from east-central Guangxi to Hunan were generally elongate in shape and arranged roughly in a NNE–SSW direction (Fig. 1), following the orientation of the major fault zones. These platforms commonly exhibited an asymmetrical profile with a sharp transition from platform to basin on the western margin, but a relatively gentle slope on the eastern margin (Tan *et al.*, 1987; Wu *et al.*, 1987; Zhong *et al.*, 1992). Reef or shoal complexes were commonly developed on western or southern margins, possibly related to the SW-trending wind direction (Shen *et al.*, 1987, 1994; Shen & Yu, 1996; Shen & Zhang, 1997). The eastern, leeward margin was generally a distally steepened ramp with progradation towards the interplatform basin (Fig. 6). This depositional configuration is different from the Devonian in the Great Basin region of the USA (a ramp system) (Dorobek, 1991; Elrick, 1995, 1996; LaMaskin & Elrick, 1997), but similar to that in western Canada and Europe (Burchette, 1981; Walls, 1983; Wendte, 1992).

Facies analysis from three isolated platforms (GX, GL and GZL) has revealed that extensive organic buildups with minor peritidal facies were deposited in the lower Givetian, corresponding to the the Tangjiawan Formation. Peritidal facies were widely distributed from late Givetian to earliest Frasnian time, but then decreased in volume until the end of the Frasnian. There are relatively large volumes of subtidal facies at localities MA and XZ, and physiographically these two localities were located close to the eastern margin of the GX platform, particularly the MA section. At TJ, the special 'tentaculitid' wackestone/packstone lithofacies is interpreted as a deposit of a semi-restricted deep subtidal environment. At FH, carbonate platform facies are intercalated with thin, deep subtidal units in the Givetian, but rapidly pass up into basinal siliceous and pelagic carbonate facies in the Frasnian. At LT, the dominant peritidal facies in the Frasnian are the shallowest of the measured sections.

In all measured sections, depositional facies are characterized by micrite-rich deposits dominated by wackestone/mudstone textures; wave and current structures such as cross-bedding, ripples and scours are rare; and only several layers of

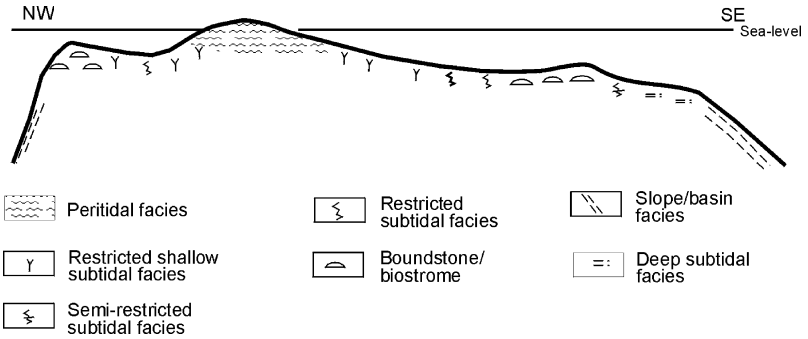

Fig. 6. Depositional model of platforms in the study area. The platforms generally exhibit a sharp transition from platform to basin on the western side over a very short distance, and a relatively gentle slope on the eastern side. Reef and shoal complexes were commonly developed on the western margin, and biostromes on the eastern side. These platforms can basically be thought of as eastward-dipping structures with distally steepened margins, which were developed on tilt-fault blocks in an extensional tectonic regime.

oolitic grainstone have been observed. This implies that the depositional facies package was deposited in a low-energy regime as a result of either wave-dampening caused by the interconnected basin system, or the effect of wave reduction by the reefs and shoals on the western sides of the platforms. Low-energy conditions across platforms resulted in highly bioturbated, homogenized subtidal deposits and tidal-flat mudstones.

HIGH-FREQUENCY CYCLICITY OF METRE-SCALE, UPWARD-SHALLOWING CYCLES

Types of metre-scale cycle

Peritidal facies through deep subtidal/basinal facies (Table 1) are organized into metre-scale, upward-shallowing cycles averaging 1·5–3·0 m thick, lasting 20–100 kyr (Tables 2 and 3). Cycle boundaries vary from abrupt to transitional. Based on the intracycle facies arrangement and features of bounding surfaces, two kinds of cycle are recognized: *peritidal cycles*, capped by peritidal facies, and *subtidal cycles*, capped by shallow through intermediate subtidal facies. The peritidal cycles are the most common (Table 2).

Peritidal cycles

Peritidal cycles are characterized by upward-shallowing successions (intermediate subtidal or restricted subtidal to peritidal facies) capped by peritidal facies (Figs 3A and 5A,B). Two subtypes of peritidal cycle are recognized: *regressive-prone* or *asymmetrical cycles*, and *transgressive-prone* or *symmetrical cycles*. Regressive-prone or asymmetrical cycles are regressive (upward-shallowing) facies successions commencing with intermediate subtidal, restricted subtidal or peritidal facies, and are capped by peritidal facies with an obvious facies 'jump' across bounding surfaces; that is, there is an abrupt deepening above cycle boundaries (Fig. 3A).

Transgressive-prone or symmetrical cycles are characterized by laminite bases followed by normal regressive (upward-shallowing) successions with gradual facies changes across the bounding surfaces (Fig. 5A). The basal transgressive laminite is basically similar to the capping laminite but with an increase in bioturbation, lamina thickness and darkness of colour, and a

Table 2. Statistics of cycle distribution in measured sections, Hunan and Guangxi provinces.

Locality	Total thickness (m)	Total cycle number	Mean cycle thickness (m)	Peritidal cycles	Subtidal cycles
Ma'anshan	694·50	250	2·78	144 (57·6%)	106 (42·4%)
Xizhaikou	399·85	207	1·93	113 (54·1%)	94 (45·9%)
Tangjiawan	530·72	271	1·96	195 (72.0%)	76 (28.0%)
Litang	410·87	249	1·65	218 (87·6%)	31 (12·4%)
Fuhe	130·28	76	1·71	39 (51.3%)	37 (48·7%)

Table 3. Estimation of cycle duration for the measured sections. Carbonate deposition at Ma'anshan and Xizhaikou began approximately one conodont zone later in the Givetian (~0·5 Myr) and at Tangjiawan half a conodont zone later (~0·25 Myr), compared with the southern part of Guangxi Province, where deposition started at the beginning of the Givetian. The time-scale is based on the data of Odin *et al.* (1982), Palmer (1983), Harland *et al.* (1989) and Fordham (1992) respectively.

	Time-scale	Ma'anshan	Xizhaikou	Tangjiawan	Litang	
Givetian	5, 6, 3·5, 4·8 Myr	128	106	>148		Cycle number
		23·4–43·0 kyr	28·3–51·9 kyr	22·0–38·9 kyr		Cycle duration
Frasnian	10, 7, 10·5, 8·7 Myr	~105	96	~128	114	Cycle number
		66·7–100 kyr	72·9–109·4 kyr	54·7–82·0 kyr	61·4–92·1 kyr	Cycle duration
		53·7–62·2 kyr	61·9–71·8 kyr	33·9–39·2 kyr		Mean cycle duration

decrease in the degree of exposure. The laminae have a wavy, undulatory appearance.

Subtidal cycles

Two varieties of subtidal cycle are recognized: *shallow subtidal cycles*, characterized by upward-shallowing successions composed of intermediate subtidal, restricted (or semi-restricted) subtidal to shallow subtidal facies (Figs 3A, and 5C and D), and *deep subtidal cycles,* upward-shallowing successions composed of deep to intermediate subtidal facies (Fig. 5E).

Shallow subtidal cycles are incomplete cycles, because the available accommodation space from the seafloor to sea-level was not fully filled. Their occurrence indicates that the accommodation increase was faster than sediment aggradation. They are present across platforms mainly within overall transgressive deposits. These cycles are basically upward-shallowing cycles without obvious evidence of prolonged subaerial exposure; only a tiny proportion exhibits features of subaerial exposure (e.g. *in situ* breccias and microkarst) at cycle tops in the lower part of the Upper Member of the Guilin Formation at TJ, Guilin. This situation more commonly occurred in cycles composed of biostrome facies as a result of their relatively high relief from the seafloor, or as the result of a sharp fall in relative sea-level. The thickest of all cycles, up to 15 m, is of this type.

Deep subtidal cycles are rare, and are only observed at the bottom of the Qizhiqiao Formation (or its equivalent) and at several horizons at FH. They are characterized by micrite-rich deposits with thin storm-generated layers and a deep-water biota, such as tentaculitids, in the lower parts of the cycles, representing low-energy conditions below fair-weather wave base. They are present mainly within overall transgressive deposits along platform margin slopes or in interplatform basins.

Cyclicity of metre-scale, upward-shallowing cycles

It is difficult to determine cycle duration from thick platform carbonate successions as a result of a lack of accurate radiometric age data and the 'missed beat effect' (cf. Goldhammer *et al.*, 1990). Here only an approximate estimation of cycle duration (Table 3) can be made with the given time-scale of the Givetian and Frasnian (Odin *et al.*, 1982; Palmer, 1983; Harland *et al.*, 1989; Fordham, 1992). It would appear that cycles in the Givetian are in the range 20–52 kyr, whereas those in the Frasnian were longer, in the range 50–110 kyr. If the deposits in the Givetian and Frasnian are taken as a whole, the cycle duration is in the range 30–72 kyr (the bottom row of Table 3). If 'missed beats' (subaerial exposure and deep subtidal missed beats) are taken into account, the cycle durations would be shorter than these estimated values. As with most metre-scale carbonate cycles, these Devonian ones are within the Milankovitch band, corresponding to fourth-and fifth-order cycles (cf. Goldhammer *et al.*, 1993).

The origin of metre-scale, carbonate cycles is still a controversial topic, provoking much debate (e.g. Drummond & Wilkinson, 1993a,b; Wilkinson *et al.*, 1996, 1997). Three mechanisms are commonly cited to explain the repetition: (1) autocyclic generation (e.g. Pratt & James, 1986; Cloyd *et al.*, 1990; Satterley, 1996), (2) episodic subsidence (e.g. Cisne, 1986; Hardie *et al.*, 1991), and (3) high-frequency, glacio-eustatic fluctuations in sea-level (e.g. Goodwin & Anderson, 1985; Goldhammer *et al.*, 1990, 1993; Balog *et al.*, 1997; Strasser & Hillgärtner, 1998).

Although all three mechanisms cited above are possible driving forces for cycle formation, the glacio-eustatic model does best explain the features of these Devonian cycles. Exposure-capped peritidal cycles are interpreted as the result of high-frequency sea-level fall below the platform surface for one or several sea-level fluctuations (subaerial exposure 'missed beats'; Goldhammer *et al.*, 1990; Elrick, 1995). Subtidal cycles, correlative with updip peritidal cycles, reflect the increased accommodation space downdip created by high-frequency sea-level rise and differential subsidence, without complete filling of the space before the ensuing sea-level rise. Symmetrical cycles with transgressive laminite bases are more probably related to symmetrical and low amplitude sea-level oscillations, allowing a degree of keep-up in the early transgressive part of a new cycle, and favouring the deposition of transgressive laminites (cf. Koerschner & Read, 1989). Glacio-eustasy is also indirectly supported by the evidence of continental glaciation in the Late Devonian (Caputo & Crowell, 1985). However, widespread exposure horizons in the lower Frasnian platform strata are more probably tectonically controlled as suggested by the presence of nearly synchronous siliceous rocks in basins and megabreccias at basin margins (discussed later).

CYCLE STACKING PATTERNS AND DEPOSITIONAL SEQUENCES

In structurally isolated and deformed shallow-water carbonate outcrops with high-frequency cycles, it is difficult to use the traditional sequence stratigraphic approach to determine the depositional sequences in view of the lack of recognizable seismic-scale stratal geometries. However, one-dimensional stratal data, including vertical cycle stacking patterns and systematic facies changes, can be used.

Cycle stacking patterns and accommodation change

The vertical stacking patterns of metre-scale, upward-shallowing cycles are mostly controlled by long-term changes in accommodation space; therefore they bridge the gap from individual cycles to the larger-scale depositional sequences, and permit the identification of sequences and their component systems tracts (e.g. Goldhammer *et al.*, 1990, 1993; Osleger & Read, 1991; Elrick, 1995).

Fischer plots are useful graphical tools to illustrate vertical stacking patterns and long-term changes in accommodation space (Fischer, 1964; Read & Goldhammer, 1988; Sadler *et al.*, 1993), particularly for peritidal cycle packages. There is, however, some dispute over the usefulness of this method to identify long-term changes of accommodation space (Drummond & Wilkinson, 1993a,b). Basically, the cycle thickness is a reflection of changes in accommodation space, but the relationship is complicated by many factors such as quasi-periodicity of cycles, variable sedimentation rates, incomplete shallowing to sea-level, non-linear subsidence rates, and missed beats. However, if extra information is included, the above negative effects can be mitigated. Fischer plots are conventionally drawn by cumulative departure from mean cycle thickness against cycle number (no less than 50) (e.g. Sadler *et al.*, 1993). In this way, thick cycle packages will positively deviate from the mean cycle thickness, and form the rising limbs of the plots, reflecting a long-term increase in accommodation space; whereas thin cycle packages will negatively deviate from the average cycle thickness, and form the falling limbs, reflecting a long-term decrease in accommodation space (Figs 7 and 8). In a more objective way, Fischer plots can be constructed with cumulative departure from mean cycle thickness against cycle thickness (e.g. Fig. 9); however, the long-term trend in this modified Fischer plot shows little difference from the conventional plot, just with a more gentle rising limb and a steeper falling limb. Precautions still need to be kept in mind when applying Fischer plots to the interpretation of subtidal cycles, although there are cases where such plots have been used successfully to predict long-term changes in accommodation space for subtidal cycles (e.g. Osleger, 1991; Osleger & Read, 1991). For deep subtidal cycles, the opposite trend may occur in the Fischer plot (i.e. the lower part of Figs 7 and 8), if the sedimentation rate is low and the water depth is too deep for the sediments to record the accommodation created by high-frequency, low-amplitude sea-level fluctuations (deep subtidal missed beats). Because this kind of cycle only comprises a small part of the succession and peritidal cycles dominate (Table 2), the effect of this 'subtidal cycle syndrome' is minimal. Even at section FH, where facies are dominated by deep-water packages with numerous 'subtidal missed beats', the trend of accommodation changes (below the Liujiang Formation), although not the true reflection, can still be displayed with the Fischer plot (Fig. 9). Moreover, the capping facies of most subtidal cycles is a very shallow-water facies (i.e. *Amphipora* wackestone/packstone), so that the cumulative lost information with a Fischer plot is not significant, especially in view of the intercalation with peritidal cycles.

In order to alleviate the shortcomings and increase the reliability of a single Fischer plot in predicting changes in accommodation space, other evidence such as vertical facies changes and stratigraphic distribution of subaerial exposure indicators have been integrated for the present study. Histograms of percentage of peritidal facies per cycle have been constructed, and compared with the Fischer plots drawn from measured sections (MA, XZ, TJ and LT). Major subaerial exposure horizons and deep subtidal facies indicators, such as black shale or nodular limestone, are also labelled on the Fischer plots (Figs 7 and 8). This approach integrates the Fischer plot of individual sections with the data of vertical facies changes to provide more exact information for long-term changes in accommodation space.

Sequence identification and correlation in platform carbonates

Sequence boundaries are the keys to determine third-order depositional sequences. Detailed

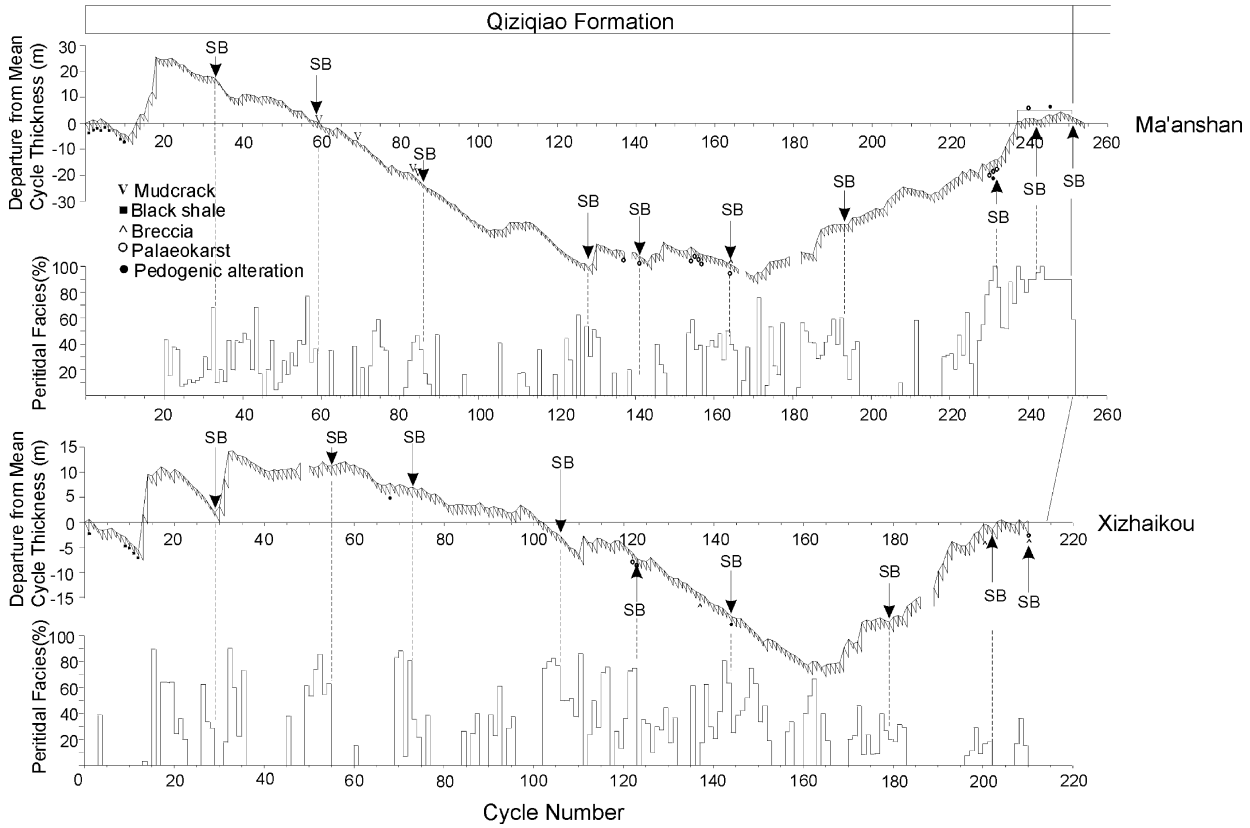

Fig. 7. Fischer plots of high-frequency metre-scale carbonate cycles combined with histograms showing percentage of peritidal facies per cycle in the Qiziqiao Formation (Givetian to Frasnian) at Ma'anshan and Xizhaikou. Major subaerial exposure features are labelled on the Fischer plots. The gaps within the curves are areas of no exposure in the field. Sequence boundary identification is mainly based on the cycle stacking patterns (on descending limbs of the plot), vertical facies variations (i.e. where high percentages of peritidal facies occur) combined with exposure indicators. Sequence boundaries (SB) are generally transitional zones.

outcrop study revealed that sequence boundaries are generally gradational over metres to tens of metres. These transitional boundaries are conformable stratigraphic zones composed of stacked, high-frequency and thinner-than-average cycles with upward-increasing intensity of subaerial exposure, rather than discrete, laterally traceable surfaces defining the sequences (e.g. Goldhammer *et al.*, 1990, 1993; Elrick & Read, 1991; Elrick, 1995). These stacked exposure-capped cyclic successions represent platforms affected by multiple episodes of subaerial exposure formed by high-frequency (fourth- to fifth-order) sea-level fluctuations superimposed on long-term (third-order) sea-level lowstands, rather than a single, long-lasting exposure event. Therefore, the sequence boundary zones should lie roughly halfway down to the lowest points on the falling-limb sections of Fischer plots, representing the maximum rate of accommodation loss. However, a more exact location of the sequence boundaries is largely dependent on the evidence from vertical facies changes, i.e. the shallowest facies association with a relatively high percentage of peritidal facies and obvious subaerial exposure indicators; these sequence boudaries are labelled in Figs 7 and 8.

Individual sequences are generally 15–90 m thick, and consist of 15–50, metre-scale, upward-shallowing cycles. The number of cycles is less within the sequences of section FH, where more deeper-water subtidal facies predominate (Fig. 9), and there may have been numerous subtidal missed beats. Internally the sequences are basically composed of a transgressive lower part and a regressive upper part (Figs 7 and 8). The transgressive deposits consist of thicker-than-average, upward-thickening cycles dominated by subtidal facies, and the regressive deposits consist of thinner-than-average, upward-thinning cycles dominated by peritidal facies. The transition between transgressive and regressive packages is gradational, so the maximum flooding surface of each sequence is tentatively placed at the mid-

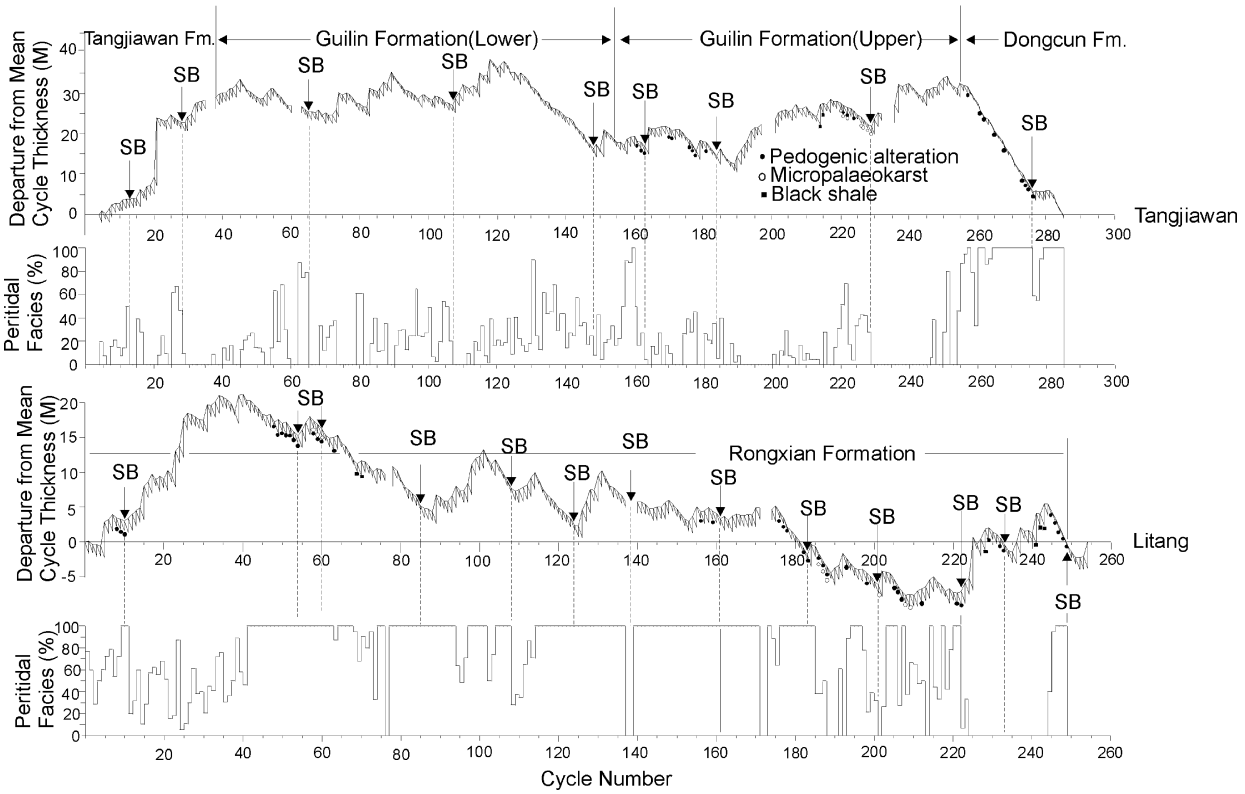

Fig. 8. Fischer plots of high-frequency carbonate cycles and facies distribution (histograms showing percentage of peritidal facies per cycle) of Givetian and Frasnian strata from the Tangjiawan (including Tangjiawan, Guilin and lower Dongcun formations) and Litang sections. Gaps on the plot are covered stratigraphic intervals in the field. The Litang section is dominated by the shallowest, peritidal deposits in these measured sections, and the Frasnian–Famennian boundary is at cycle 124. Sequence boundaries are marked with SB.

point of the thickest cycle in the vertical succession.

It is necessary to note that the bottom of the Tangjiawan Formation in the Guilin area roughly corresponds to the base of *varcus* conodont zone (Shen & Yu, 1996); and the Qiziqiao Formation in central Hunan was deposited later (approximately half a conodont zone). *Stringocephalus* (no later than *hermanni-cristatus* Zone, Shen & Yu, 1996) disappears in the third sequence above the clastics in the Guilin area, but in the second in central Hunan, so there is one sequence less at MA and XZ. The top boundary of the Qiziqiao Formation in central Hunan approximately corresponds to the base of the middle *triangularis* Zone or a little higher (Ji, 1991). A transitional unit named the Laojiangchong Member (BGMR of Hunan, 1997) exists between the Changlongjie Formation and the underlying platform carbonates (top of the Frasnian), in which two small-scale sequences have been recognized (Muchez *et al.*, 1996; Bai *et al.*, 1997). These two sequences are also recognized in the lower part of the Dongcun Formation at TJ and Wuzhishan Formation at FH. At MA and XZ, two small-scale sequences are recognized in the uppermost part of the Qiziqiao Formation (one less at XZ due to incomplete measurement of the section, Fig. 7); their base therefore corresponds to the upper boundary of the Frasnian. At LT, the Rongxian Formation is overlain by slope deposits of early Carboniferous age (with the coral *Pseudouralinia* sp.). The Frasnian–Famennian boundary is placed at the top of the sequence below the second gap (Fig. 8) through comparison with Famennian sequences elsewhere (e.g. Johnson *et al.*, 1985; Chen & Chen, 1994a; Du *et al.*, 1996). Moreover, the brachiopod *Cyrtospirifer,* an index fossil of the Upper Devonian, occurs in the seventh sequence at TJ, and the sixth at MA and XZ, or a little lower. Futhermore, the Frasnian–Famennian event with its dramatic biotic and sedimentological changes, is also used to define the top boundary of the Frasnian.

From Givetian through Frasnian strata, nine sequences and sequence boundary zones can be recognized. However, at the MA and XZ sections there is one sequence less, attributable to the later

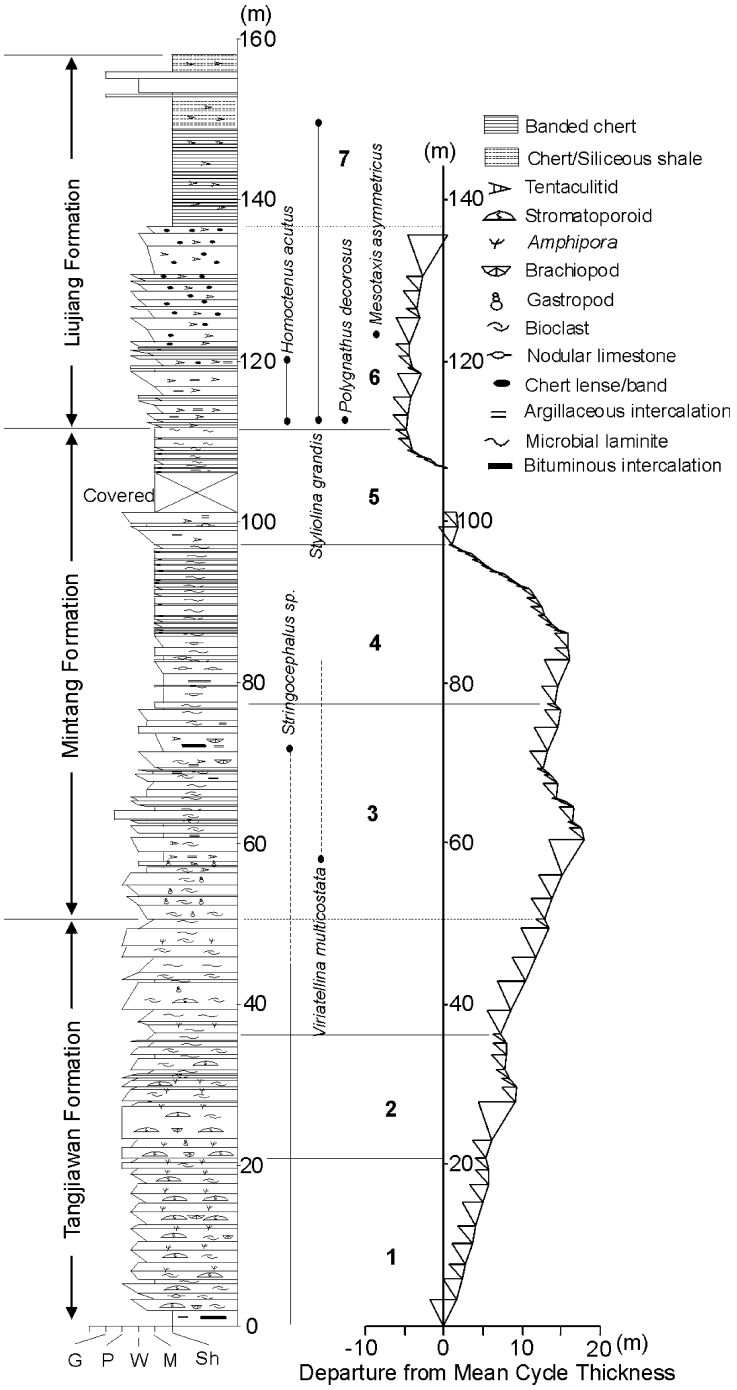

Fig. 9. Stratigraphic column from Givetian to lower Frasnian strata at Fuhe (with fossil assemblage data for the age definition). The right saw-like curve is a modified Fischer plot drawn with the cumulative departure from mean cycle thickness against cycle thickness, in order to fit to the stratigraphic log. Episodic deepening interrupted by microbial laminite intervals in the Mintang Formation (Givetian) are followed by a rapid deepening at the base of the Liujiang Formation (latest Givetian to early Frasnian), recording a long-term accelerating accommodation gain at this time. The Fischer plot does not correlate very well with the accommodation changes recorded on the platform, especially from the upper part of the Mintang Formation (just above the covered interval), as a result of the effect of deeper-water sedimentation and 'subtidal missed beats', when water depth was too deep to respond to small-scale, high-frequency sea-level changes. Sh, shale; M, mudstone; W, wackestone; P, packstone; G, grainstone.

start of deposition in the early Givetian. The correlation of these sequences is given in Fig. 10, based on internal facies organization, progressive facies change and the biostratigraphic framework.

Sequence 1 is the first carbonate sequence overlying clastic strata and is only developed in Guilin and farther south, because the Devonian marine transgression started from the southern area of Guangxi, and gradually extended northward. The internal succession is dominated by subtidal cycles (including many dolomitized biostromes of stromatoporoid boundstone/rudstone) with minor peritidal cycles above.

Sequence 2 is recognized from Guangxi up to Hunan. Transgressive deposits are characterized by thick subtidal cycles with many biostromes, particularly in the upper part, and are also strongly dolomitized. Some deep subtidal cycles are observed in the lower part of the sequences at localities MA and XZ, and show a falling pattern

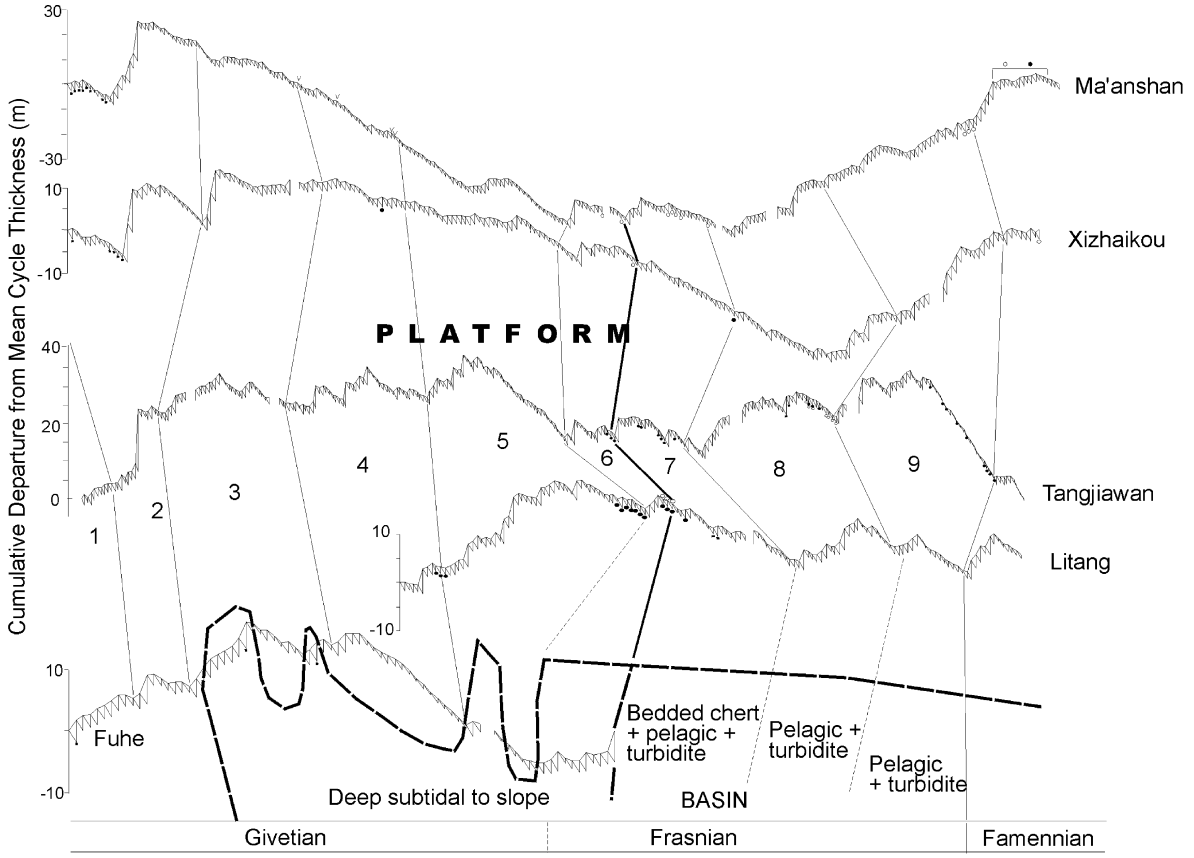

Fig. 10. Correlation of Fischer plots between outcrops from three isolated carbonate platforms in Hunan and Guangxi provinces. Nine sequences (third-order) were identified in Givetian and Frasnian strata, of which the lower five sequences (Sequence 1–5) are Givetian, and the upper four sequences (Sequence 6–9) are Frasnian. There is a long-term reduction in accommodation space from Sequence 3–6 in the platform successions, but an opposite trend is observed in the interplatform basin successions, as at Fuhe. The trend in the Fischer plot from Sequence 6 at Fuhe is not a true reflection of accommodation change, but is a result of deeper-water sedimentation and the ''subtidal missed beats'' effect; deep-water facies are indicated below the dashed line. The thicker line between Sequence 6 and 7 is the most obvious boundary with widespread subaerial exposure. See Figs 7 and 8 for legend.

on the Fischer plots; this is the result of the low sedimentation rate and/or compacted clay-rich horizons within the cycles. Sequences 1 and 2 were deposited at a time of rapidly increasing accommodation space.

Sequences 3–7 record a long-term change from a slow to a rapid decrease in the amount of accommodation space available. Sequences 3–5 contain relatively high numbers of peritidal cycles; subtidal cycles are concentrated within the lower transgressive parts, and generally are highly dolomitized. Prolonged exposure is only recorded towards the top of Sequence 5 in the shallowest succession at LT (Figs 5A and 8). Sequence 6 is the thinnest of the sequences in each section, ranging from 15 to 30 m in thickness, indicating the smallest amount of accommodation space. Exposure events represented by pedogenic and palaeokarstic horizons are observed towards the top of this sequence in almost all localities (Figs 7, 8 and 10). These exposure events occur locally at the top of subtidal cycles, indicating that their formation was abrupt and prolonged. These long-lasting periods of exposure and lack of accommodation space prevented further deposition on the platforms, and resulted in the absence of a regressive, upper part to Sequence 6. Sequence 7 is transitional and shows an increase in the volume of subtidal facies and in the thickness of the sequence, indicating a decrease in the rate of accommodation loss. However, the significant loss of accommodation space at the end of Sequence 6 still had an obvious impact on the deposition of this sequence; the exposure events observed locally in the middle part of this sequence indicate that there was abrupt exposure or insufficient accommodation space across the platforms (Fig. 10). By

contrast, at FH, evidence for sporadic and gradual deepening is recorded in Sequences 3 through 5, and sudden deepening is recorded in Sequence 6, with the deepest water facies occurring in the lower part of Sequence 7 (Fig. 9).

Sequences 8 and 9 record a long-lasting, rapid increase in accommodation space with relatively thick cycles. The volume of subtidal facies increases and peritidal facies decreases through the sequences. Even the peritidal facies packages show an increasing degree of deepening as indicated by more fenestral limestones than laminites, particularly in Sequence 9. The top of Sequence 9 roughly corresponds to the boundary between the Frasnian and Famennian, which occurs in the Qiziqiao, Dongcun and Rongxian formations.

Sequence stacking patterns

The sequences identified from cycle stacking patterns and vertical facies changes can be roughly grouped into two categories: *catch-up sequences* and *keep-up sequences* (Fig. 10).

Catch-up sequences (Sequences 1–2 and 8–9) are characterized by packages of relatively thick cycles with a high percentage of intermediate to shallow subtidal facies, and even deep subtidal facies locally within individual cycles. These form the ascending wave trains on the Fischer plots and indicate a long-term (second-order) increase in accommodation space. These sequences are dominated by subtidal cycles, particularly in the lower transgressive part of the sequences, and minor peritidal cycles occur in the more regressive, upper part. These features indicate that sedimentation rates on platforms were slower than the accommodation gains created by the combined effects of fifth- through third-order relative sea-level changes, enhanced by the second-order, long-term relative sea-level rise.

Keep-up sequences (Sequences 3–6) are characterized by relatively thin cycle packages with a high percentage of peritidal facies within individual cycles. These form the descending limbs on the Fischer plots and indicate a long-term (second-order) accommodation decrease. At localities MA and XZ, there are no obvious rising limbs even in the transgressive deposits within these sequences. Subtidal cycles are only found in the transgressive deposits, and exposure-capped peritidal cycles become more common towards the top of the sequences. Furthermore, in Sequence 6 the upper part of the regressive deposits are mostly absent because of the stacked, prolonged subaerial exposure events towards the top. These characteristics indicate that the sedimentation rate on the platform generally kept pace with accommodation gain created by the combined effects of fifth- through third-order relative sea-level changes, attenuated by a second-order, long-term relative sea-level fall. The combined effects caused a maximum rate of accommodation loss on the platforms at the end of Sequence 6. Sequence 7 is transitional (i.e. deposited during a period of long-term stillstand) with characteristics of both keep-up and catch-up platform sequences.

Within interplatform basinal successions (e.g. Wu *et al.*, 1987; Jin, 1990), such as at locality FH (Fig. 9), a widespread deepening process was started from Sequence 6, with the deepest water represented by pelagic, hemipelagic and siliceous facies in the lower part of Sequence 7, after which the water depth became shallow.

Long-term changes in cycle stacking patterns and tectonic implications

Long-term changes in cycle stacking patterns and accommodation in these Devonian platform carbonates are well illustrated with the Fischer plots (Figs 7, 8 and 10). Although there are some differences, comparison of Fischer plots constructed from sections located on different platforms reveals a similar pattern (Fig. 10), suggesting similar, long-term trends in accommodation change. In these platform successions, a rapid increase in accommodation space during the early Givetian (Sequences 1–2) was followed by a gradual to rapid decrease in accommodation space from the middle to late Givetian (Sequences 3–5), reaching a maximum rate of accommodation loss in the early Frasnian (the top of Sequence 6). Afterwards, the accommodation space change was uniform or increased slightly (Sequence 7); this was followed by a rapid increase until the end of the Frasnian (Sequences 8–9). In detail, small differences in accommodation change are present between individual platforms, as can be seen from the Fischer plots of localities MA and XZ (both on platform GX) when compared with localities TJ (on platform GL) and LT (on platform GZL) (Fig. 10). These reflect small variations in the subsidence rate of the three platforms.

One significant phenomenon in Sequence 6 and 7 is that the rapid loss in accommodation space on the platforms coincided with a rapid gain in accommodation in the interplatform

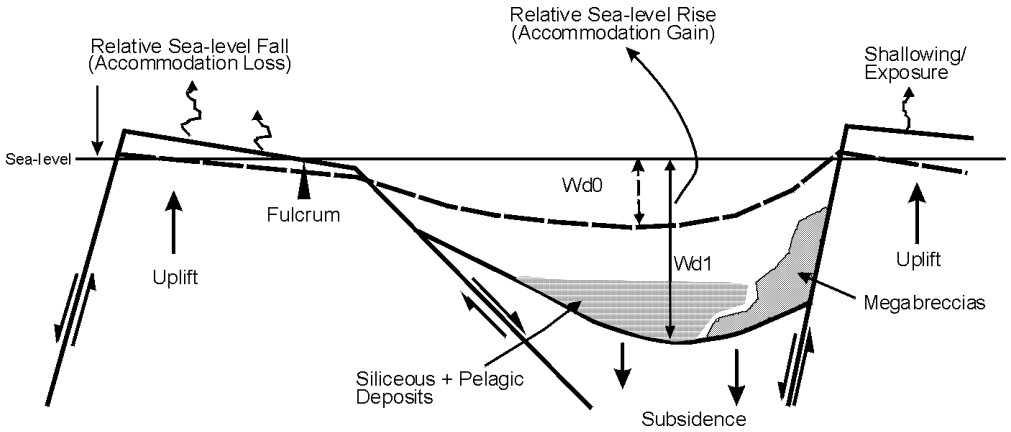

Fig. 11. Schematic diagram showing the tectonic controls on platform and interplatform basin deposition and development in an extensional regime. The rapid subsidence of interplatform basins controlled by faults would be accompanied by the relative uplift of platforms, resulting in an accommodation gain in the basins, but an accommodation loss on the platforms. The condensed exposure disconformity zones on platforms therefore correspond to sharp deepening in the basins. The arrows mark the relative movement direction of blocks. Wd0, initial water depth before fault movement; Wd1, water depth after fault movement.

basins. The sharp deepening event in the basin indicated by siliceous deposits (bedded cherts and siliceous shales) and coarse debrites at the basin margins, corresponds to the major subaerial exposure horizon between the two sequences on the platforms (Fig. 10). This opposing trend in accommodation change between platforms and basins is well demonstrated at the FH section (Fig. 9), a profile recording the transition from platform to the interplatform basin, on the eastern side of the Guilin platform.

This contrast between platforms and basins was the result of the extensional tectonic movements noted earlier, whereby rapid deepening and increase in accommodation space in basins, was accompanied by relative uplift of platforms, resulting in a large loss of accommodation there and so shallowing and subaerial exposure (Fig. 11). During the fault movements, a jerky subsidence of the basins (hanging walls) triggered slope failure, and led to the deposition of debrites and slumps, followed by deep-water pelagic deposition in the basin. The exposure disconformity zones on the platforms (at the top of Sequence 6) therefore roughly correspond to the sudden deepening event indicated by the debrites

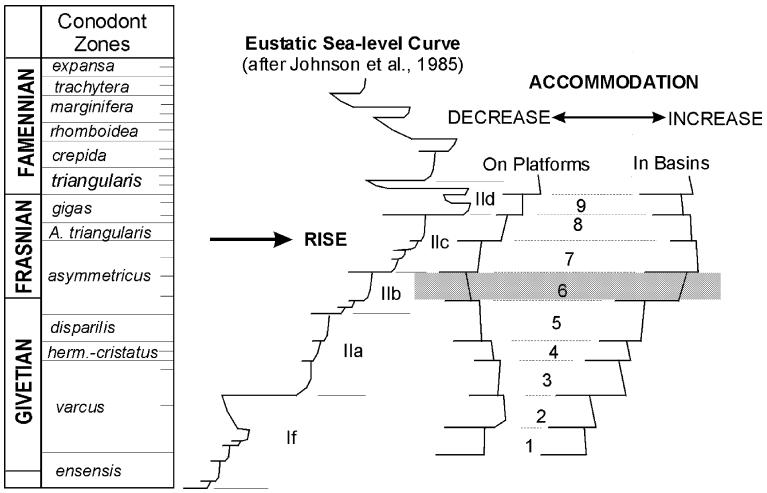

Fig. 12. Comparisons of accommodation changes on platforms and in basins in the study area with the eustatic sea-level curve constructed by Johnson *et al.* (1985), for Givetian through Frasnian strata. Numbers (1–9) are the depositional sequences documented in this paper. Note the opposite trend in accommodation changes, and the coincidence of maximum rate of accommodation loss with accommodation gain in Sequence 6 (shadowed bar) between platforms and basins. Note the broadly opposite and similar trend, respectively, for platform and basins, in accommodation changes, compared with Johnson *et al.*'s eustatic sea-level curve.

and related siliceous deposits in the basins. This opposite pattern in accommodation change is most probably related to the tectonic activity at the time.

The long-term changes in accommodation discerned from cycle stacking patterns from different platforms in South China do not show a good correlation to the pattern of eustatic sea-level change in Euramerica postulated by Johnson *et al.* (1985). In fact, an opposite trend in accommodation changes is mostly seen (Fig. 12). This suggests that local tectonics was a major factor in platform generation and evolution in South China, as seen in the opposing pattern of accommodation changes between platforms and basins in Sequences 6 and 7.

CONCLUSIONS

1 From the Middle Devonian, a complex pattern of platforms and interplatform basins was well established in South China. Five depositional facies including peritidal, restricted shallow subtidal, semi-restricted subtidal, intermediate subtidal, and deep subtidal facies, and 18 lithofacies units are recognized from measured sections located on three isolated platforms in Givetian and Frasnian successions. These deposits are arranged into metre-scale, upward-shallowing cycles grouped into peritidal and subtidal cycles, which have an average cycle period between ≈22–110 kyr. This periodicity roughly falls within the time-scale of Milankovitch rhythms, although the mechanism of cycle formation is still uncertain.

2 Nine third-order depositional sequences are identified, based on changes in cycle stacking patterns, vertical facies changes, and the stratigraphic distribution of subaerial exposure indicators. The internal components of sequences are mainly composed of lower transgressive and upper regressive parts. Transgressive packages are dominated by thicker-than-average subtidal cycles, whereas regressive parts are dominated by thinner-than-average peritidal cycles. Sequence boundaries are generally conformable, transitional zones composed of stacked, high-frequency, and thinner-than-average cycles with upward-increasing intensity of subaerial exposure, rather than discrete, laterally traceable surfaces.

3 The identified sequences can be further grouped into catch-up and keep-up sequence sets from the long-term (second-order) trend in accommodation space revealed by Fischer plots. Catch-up sequences (Sequences 1–2, 8–9) are characterized by packages of relatively thick cycles with a high percentage of intermediate to shallow subtidal facies, and even deep subtidal facies locally within individual cycles, recording increased rates of long-term accommodation gain. Keep-up sequences (Sequences 3–6) are characterized by packages of relatively thin cycles with a high percentage of peritidal facies within individual cycles, recording increased rates of long-term accommodation loss. This long-term sequence stacking pattern is tectonically controlled.

4 The long-term increasing accommodation loss on platforms from late Givetian to early Frasnian times coincided with increasing accommodation gain in interplatform basins. This implies that, under an extensional regime, the deepening in interplatform basins induced by increasing subsidence can be associated with the relative uplift of platforms, resulting in accommodation loss and shallowing there. The deep-water packages in basins (i.e. between Sequence 6 and 7) therefore roughly correspond to the stacked exposure disconformities on the platforms.

ACKNOWLEDGEMENTS

This research was funded by the National Natural Science Foundation of China (grant no. 49404023, and 49872043 to C.D.Z.). Fieldwork was generously assisted by Professors Baoan Yin, Yi Wu, and many young colleagues in the Regional Geological Survey of Guangxi at different times. We are very grateful to the K. C. Wong Education Foundation and the Royal Society for the support to the senior author to visit Durham University for one year. Thanks also go to the Institute of Geology & Geophysics, Chinese Academy of Sciences, for allowing the senior author's research absence from the Institute during the tenure of the Fellowship. The manuscript has benefited greatly from reviews by Maya Elrick and Bruce Wilkinson. Numerous constructive editorial comments from Dr Ian Jarvis are highly appreciated.

REFERENCES

Bai, S.L., Bai, Z.Q., Ma, X.P., Wang, D.R. and **Sun, Y.L.** (1997) *Devonian Events and Biostratigraphy of South China*. Peking University Press, Beijing, China. pp. 62–113.

Balog, A., Haas, J., Read, J.F. and **Coruh, C.** (1997) Shallow marine record of orbitally forced cyclicity in a Late

Triassic carbonate platform, Hungary. *J. Sed. Res.*, **67,** 661–675.

Burchette, T.P. (1981) European Devonian reefs: a review of current concepts and models. In: *European Fossil Reef Models* (Ed. D.F. Toomey), *SEPM Spec. Publ.*, **30,** 85–142.

Bureau of Geology and Mineral Resources (BGMR) of Hunan Province (1997) *Multiple Classification and Correlation of the Stratigraphy of China (43) – Stratigraphy (Lithostratigraphy) of Hunan Province.* China University of Geoscience Press, Wuhan, China. pp. 123–160.

Caputo, M.V. and **Crowell, J.C.** (1985) Migration of glacial centers across Gondwana during Paleozoic Era. *Geol. Soc. Am. Bull.*, **96,** 1020–1036.

Chen, D.Z. and **Chen, Q.Y.** (1994a) Devonian sedimentary evolution and transgressive-regressive patterns in South China. *Sci. Geol. Sinica*, **29,** 246–255 (in Chinese with English abstract).

Chen, D.Z. and **Chen, Q.Y.** (1994b) Sequence stratigraphic frameworks and sea-level changes of Early and Middle Devonian, southern Guizhou. *Sci. Sinica (Series B)*, **24,** 1197–1205 (in Chinese).

Chen, D.Z. and **Chen, Q.Y.** (1995) Dynamics of sedimentary evolution for the Early and Middle Devonian, southern Guizhou. *Acta Sedimentol. Sinica*, **13,** 54–65 (in Chinese with English abstract).

Chen, H.D. and **Zeng, Y.F.** (1990) Nature and Evolution of the Youjiang Basin. *Sed. Facies Palaeogeogr.*, **1,** 28–37 (in Chinese with English abstract).

Cisne, J.L. (1986) Earthquakes recorded stratigraphically on carbonate platforms. *Nature*, **323,** 320–322.

Cloyd, K.C., **Demicco, R.U.** and **Spencer, R.J.** (1990) Tidal channel, levee, and crevasse splay deposits from a Cambrian tidal channel system – a new mechanism to produce shallowing-upward sequences. *J. Sed. Petrol.*, **60,** 73–83.

Deconinck, J.-F. and **Strasser, A.** (1987) Sedimentology, clay mineralogy and depositional environments of Purbeckian green marls (Swiss and French Jura). *Eclogae Geol. Helv.*, **80,** 753–772.

Dorobek, S.L. (1991) Cyclic platform carbonates of the Devonian Jefferson Formation, southwestern Montana. In: *Paleozoic Paleogeography of the Western United States-II* (Eds J.D. Cooper and C.H. Stevens), *SEPM Pacific Section*, **67,** 509–526.

Drummond, C.N. and **Wilkinson, B.H.** (1993a) Aperiodic accummulation of peritidal carbonates. *Geology*, **21,** 1023–1026.

Drummond, C.N. and **Wilkinson, B.H.** (1993b) On the use of cycle thickness diagrams as records of long-term sea-level change during accummulation of carbonate sequences. *J. Geol.*, **101,** 687–702.

Du, Y.S., **Gong, Y.M.** and **Wu, Y.** (1996) Devonian sequence stratigraphy and sea-level change cycles in South China. *J. China Univ. Geosci.*, **7,** 72–79.

Elrick, M. (1995) Cyclostratigraphy of Middle Devonian carbonates of the eastern Great Basin. *J. Sed. Res.*, **B65,** 61–79.

Elrick, M. (1996) Sequence stratigraphy and platform evolution of Lower-Middle Devonian carbonates, eastern Great Basin. *Geol. Soc. Am. Bull.*, **108,** 392–416.

Elrick, M. and **Read, J.F.** (1991) Cyclic ramp-to-basin carbonate deposits, Lower Mississippian, Wyoming and Montana: a combined field and computer modeling study. *J. Sed. Petrol.*, **61,** 1194–1224.

Fischer, A.G. (1964) The Lofer cyclothems of the Alpine Triassic. In: *Symposium of Cyclic Sedimentation* (Ed. D.F. Merriam), *Bull. Kansas Geol. Surv.*, **169,** 107–149.

Fordham, B.G. (1992) Chronometric calibration of mid-Ordovician to Tournaisian conodont zones: a compilation from recent graphic-correlation and isotope studies. *Geol. Mag.*, **129,** 709–721.

Garland, J., **Tucker, M.E.** and **Scrutton, C.T.** (1996) Microfacies analysis and metre-scale cyclicity in the Givetian backreef sediments of south-east Devon. *Proc. Ussher Soc.*, **9,** 31–36.

Goldhammer, R.K., **Dunn, P.A.** and **Hardie, L.A.** (1990) Depositional cycles, composite sea-level changes, cycle stacking patterns, and the hierarchy of stratigraphic forcing: Examples from platform carbonates of the Alpine Triassic. *Geol. Soc. Am. Bull.*, **102,** 535–562.

Goldhammer, R.K., **Lehmann, P.J.** and **Dunn, P.A.** (1993) The origin of high-frequency platform carbonate cycles and third-order sequences (Lower Ordovician El Paso Group, west Texas): Constraints from outcrop data and statigraphic modeling. *J. Sed. Petrol.*, **63,** 318–360.

Gong, Y.M., **Wu, Y.**, **Du, Y.S.**, **Feng, Q.L.** and **Liu, B.P.** (1997) The Devonian sea-level change rhythms in South China and coupling relationships of the spheres of the Earth. *Acta Geol. Sinica*, **71,** 212–226 (in Chinese with English abstract).

Goodwin, P.W. and **Anderson, E.A.** (1985) Punctuated aggradational cycles: a general hypothesis of stratigraphic accumulation. *J. Geol.*, **93,** 515–533.

Hardie, L.A., **Dunn, P.A.** and **Goldhammer, R.K.** (1991) Field and modeling studies of Cambrian cycles, Virginian Appalachians – Discussion. *J. Sed. Petrol.*, **61,** 636–646.

Harland, W.B., **Armstrong, R.L.**, **Cox, A.V.**, **Craig, L.E.**, **Smith, A.G.** and **Smith, D.G.** (1989) *A Geological Time Scale.* Cambridge University Press, Cambridge.

Ji, Q. (1991) Conodont biostratigraphy and mass extinction event near the Frasnian–Famennian boundary in south China. *Bull. Chin. Acad. Geo. Sci.*, **23,** 115–127 (in Chinese with English abstract).

Jiang, D.H. (1990) Sedimentary characteristics and evolution of Middle and Late Devonian interplatform basin in southern Hunan. *Sed. Facies Palaeogeogr.*, **6,** 21–29 (in Chinese with English abstract).

Jin, Y.J. (1990) The diachronism of the Dinghechong Formation. *J. Stratigr.*, **14,** 131–135 (in Chinese).

Johnson, J.G., **Klapper, G.** and **Sandberg, C.A.** (1985) Devonian eustatic fluctuations in Euramerica. *Geol. Soc. Am. Bull.*, **96,** 567–587.

Koerschner, W.F. and **Read, J.F.** (1989) Field and modelling studies of Cambrian carbonate cycles, Virginia Appalachians. *J. Sed. Petrol.*, **59,** 654–687.

Lamaskin, T. and **Elrick, M.** (1997) Sequence stratigraphy of the Middle to Upper Devonian Guilmette Formation, southern Egan and Schell Creek ranges, Nevada. In: *Paleozoic Sequence Stratigraphy, Biostratigraphy, and Biogeography: Studies in Honor of J. Granville ('Jess') Johnson* (Eds G. Klapper, M. A. Murphy and J. A. Talent), *Geol. Soc. Am. Spec. Pap.*, **321,** 89–112.

Liu, W.J. (1998) Evolution of sedimentation on the South China Plate in the Hercynian-Indosinian stage. *J. Chengdu Univ. Technol.*, **25,** 328–336 (in Chinese with English abstract).

Liu, W.J., **Zhang, J.Q.** and **Chen, H.D.** (1993) Geological features of Devonian sedimentary basins in South China and their deposition and mineralization. *Acta Geol. Sinica*, **67,** 244–254 (in Chinese with English abstract).

McLean, D.J. and **Mountjoy, E.W.** (1994) Allocyclic control on Late Devonian buildup development, southern Canadian Rocky Mountains. *J. Sed. Res.*, **B64,** 326–340.

Montañez, I.P. and **Read, J.F.** (1992) Eustatic control on early dolomitization of cyclic peritidal carbonates: Evidence from the Early Ordovician Upper Knox Group, Appalachians. *Geol. Soc. Am. Bull.*, **104,** 872–886.

Montañez, I.P. and **Osleger, D.A.** (1993) Parasequence stacking patterns, third-order accommodation events, and sequence stratigraphy of Middle to Upper Cambrian platform carbonates, Bonanza King Formation, southern Great Basin. In: *Recent Advances and Applications of Carbonate Sequence Stratigraphy* (Eds B. Loucks and J. F. Sarg), *AAPG Mem.*, **57,** 305–321.

Muchez, P.H., **Boulvain, F.**, **Dreesen, R.** and **Hou, H.F.** (1996) Sequence stratigraphy of the Frasnian-Famennian transitional strata: a comparison between South China and southern Belgium. *Palaeogeogr. Palaeoclimatol. Palaeoecol.*, **123,** 289–296.

Odin, G.S., **Curry, D.**, **Gale, N.H.** and **Kennedy, W.J.** (1982) The Phanerozoic time-scale in 1981. In: *Numerical Dating in Stratigraphy* (Ed. G. S. Odin), pp. 956–960. John Wiley & Sons, New York.

Osleger, D.A. (1991) Subtidal carbonate cycles: Implications for allocyclic versus autocyclic controls. *Geology*, **19,** 917–920.

Osleger, D.A. and **Read, J.F.** (1991) Relation of eustasy to stacking patterns of meter-scale carbonate cycles, Late Cambrian, USA. *J. Sed. Petrol.*, **61,** 1225–1252.

Palmer, A.R. (1983) The decade of North American geology: 1983 geologic time-scale. *Geology*, **11,** 503–504.

Pratt, B.R. and **James, N.P.** (1986) The St. George Group (Lower Ordovician) of western Newfoundland: Tidal-flat island model for carbonate sedimentation in shallow epeiric seas. *Sedimentology*, **33,** 313–343.

Read, J.F. (1973) Carbonate cycles, Pillara Formation (Devonian), Canning Basin, Western Australia. *Bull. Can. Petrol. Geol.*, **21,** 38–57.

Read, J.F. and **Goldhammer, R.K.** (1988) Use of Fischer plots to define third-order sea level curves in peritidal cyclic carbonates, Early Ordovician, Appalachians. *Geology*, **16,** 895–899.

Sadler, R.M., **Osleger, D.A.** and **Montañez, I.P.** (1993) On the labelling, length and objective basis of Fischer plots. *J. Sed. Petrol.*, **63,** 360–369.

Satterley, A.K. (1996) Cyclic carbonate sedimentation in the Upper Triassic Dachstein Limestone, Austria: the role of patterns of sediment supply and tectonics in a platform-reef-basin system. *J. Sed. Res.*, **B66,** 307–323.

Shen, J.W. and **Yu, C.M.** (1996) Stratigraphic boundaries on Devonian carbonate platform and reef complexes in Guilin, Guangxi. *J. Stratigr.*, **20,** 1–8 (in Chinese with English abstract).

Shen, J.W. and **Zhang, S.L.** (1997) A Late Devonian (Frasnian) coral-bafflestone reef at Houshan in Gulin, South China. *Facies*, **37,** 95–108.

Shen, D.Q., **Chen, Y.Q.** and **Yang, Z.Q.** (1987) Sedimentary Facies. *Palaeogeography and Controls on Ore Deposits of the Qiziqiao Formation (Late Middle Devonian), South China.* Geological Publishing House, Beijing, China.

Shen, J.W., **Yu, C.M.**, **Yin, B.A.** and **Zhang, S.L.** (1994) Reef complexes and sequences of Devonian carbonate platforms in Guilin. *J. Stratigr.*, **18,** 161–166 (in Chinese with English abstract).

Strasser, A. (1988) Shallowing-upward sequences in Purbeckian peritidal carbonates (lowermost Cretaceous, Swiss and French Jura Mountains). *Sedimentology*, **35,** 369–383.

Strasser, A. and **Hillgärtner, H.** (1998) High-frequency sea-level fluctuations recorded on a shallow carbonate platform (Berriasian and Lower Valanginian of Mount Salev, French Jura). *Eclogae Geol. Helv.*, **91,** 375–390.

Szuczewski, M., **Belka, Z.** and **Skompski, S.** (1996) The drowning of a carbonate platform: an example from the Devonian-Carboniferous of the southwestern Holy Cross Mountains, Poland. *Sed. Geol.*, **106,** 21–49.

Tan, Z.X., **Dong, Z.C.** and **Tang, X.S.** (1987) On the Qiziqiao (Chitzechiao) Limestone. *J. Stratigr.*, **11,** 77–90 (in Chinese).

Walls, R.A. (1983) Golden Spike Reef Complex, Alberta. In: *Carbonate Depositional Environments* (Eds P. A. Scholle, D. G. Bebout and C. H. Moore), *AAPG Mem.*, **33,** 445–453.

Wendte, J. (1992) Platform evolution and its control on reef inception and localization. In: *Devonian-Early Mississippian Carbonates of the Western Canada Sedimentary Basin: a Sequence Stratigraphic Framework* (Eds J. Wendte, F. A. Stoakes and C. V. Campell), *SEPM Short Course*, **28,** 41–87.

Wilkinson, B.H., **Diedrich, N.W.** and **Drummond, C.N.** (1996) Facies succession in pertidal carbonate sequences. *J. Sed. Res.*, **66,** 1065–1078.

Wilkinson, B.H., **Drummond, C.N.**, **Rothman, E.D.** and **Diedrich, N.W.** (1997) Stratal order in peritidal sequences. *J. Sed. Res.*, **67,** 1068–1082.

Wong, P.K. and **Oldershaw, A.E.** (1980) Causes of cyclicity in reef interior sediments, Kaybob Reef, Alberta. *Bull. Can. Petrol. Geol.*, **28,** 411–424.

Wu, Y., **Zhou, H.L.**, **Jiang, T.C.**, **Fang, D.N.** and **Huang, W.S.** (1987) *The Sedimentary Facies, Palaeogeography and Relative Mineral Deposits of the Devonian in Guangxi*. Guangxi People's Publishing House, Nanning, China.

Yang, W., **Harmsen, F.** and **Kominz, M.A.** (1995) Quantitative analysis of a cyclic peritidal carbonate sequence, the Middle and Upper Devonian Lost Burro Formation, Death Valley, California – a possible record of Milankovitch climatic cycles. *J. Sed. Res.*, **B65,** 306–322.

Zeng, Y.F., **Chen, H.D.**, **Zhang, J.Q.** and **Liu, W.J.** (1992) Types and main characteristics of Devonian sedimentary basins in South China. *Acta Sedimentol. Sinica*, **10,** 104–113 (in Chinese with English abstract).

Zeng, Y.F., **Liu, W.J.**, **Chen, H.D.**, **Zheng, R.C.**, **Zhang, J.Q.**, **Li, X.Q. Li, X.Q.** and **Jiang, T.C.** (1995) Evolution of sedimentation and tectonics of the Youjiang composite basin, South China. *Acta Geol. Sinica*, **69,** 113–124 (in Chinese with English abstract).

Zhang, J.Q. and **Zheng, R.C.** (1990). *Tectonic Pattern, Lithofacies and Palaeogeography of the Devonian, Southwest Upper Yangtze Area.* Chengdu Polytechnic University Press, Chengdu, China.

Zhong, G., **Wu, Y.**, **Yin, B.A.**, **Liang, Y.L.**, **Yao, Z.G.** and **Peng, J.L.** (1992) *Devonian of Guangxi*. China University of Geoscience Press, Wuhan, China.

Manuscript received 25 November 1999;
revision accepted 9 May 2000.